

# Effects of precursor and support variation in the performance of uranium oxide catalysts for CO oxidation and selective reduction of NO

Tom Campbell<sup>a,1</sup>, Mark A. Newton<sup>a,2</sup>, Vicky Boyd<sup>b</sup>, Darren F. Lee<sup>b</sup>, John Evans<sup>a,\*</sup>

<sup>a</sup> School of Chemistry, University of Southampton, Highfield, Southampton, Hants SO17 1BJ, UK

<sup>b</sup> British Nuclear Fuels Plc, Nuclear Sciences and Technology Services, Preston, Lancashire PR4 0XJ, UK

Received 22 July 2005; received in revised form 22 September 2005; accepted 22 September 2005

Available online 24 October 2005

## Abstract

Uranium oxide catalysts supported upon  $\gamma$ -Al<sub>2</sub>O<sub>3</sub> and amorphous and mesoporous silica have been tested for CO/O<sub>2</sub> and NO/CO conversions. Pre-calcination is deleterious to catalysts on a mesoporous support due to extrusion of the active uranium phase into poorly dispersed uranium oxide particles. Developing the catalysts under CO/O<sub>2</sub>/He or CO/NO/He avoids extrusion and results in superior mesoporous catalysts (from uranyl nitrate precursor) which are comparable to Pt/Al<sub>2</sub>O<sub>3</sub> catalysts. Chloride is found generally to be deleterious to catalyst performance. The exception to this in UCl<sub>4</sub>/ $\gamma$ -Al<sub>2</sub>O<sub>3</sub> calcined at 873 K for CO/O<sub>2</sub>. In this system, the total activity is correlated to the level of chlorine retention and average uranium phase crystallite size within the catalyst. The net rate expression for selective reduction of NO by CO over the best mesoporous catalyst is zero order in NO and proportional to [CO]<sup>1.4</sup> in contrast to bulk U<sub>3</sub>O<sub>8</sub> where the net rate depends upon [NO]. The activation energy ( $E_{(a)}$ ) and pre-exponential factors ( $\nu$ ) are highly correlated both to each other and the net dispersion of the UO<sub>2.2</sub> phase recovered after catalysis; the most active systems are highly dispersed where the  $E_{(a)}$  values are more than compensated for by higher values of  $\nu$ .  
© 2005 Elsevier B.V. All rights reserved.

**Keywords:** Mesoporous; Silica; Uranium; Oxides; NO reduction

## 1. Introduction

Uranium oxide based materials are active for a wide range of total and selective oxidation processes [1–10]. These include efficient catalysts for NO<sub>x</sub> removal processes, showing a net activity comparable to Pt based catalysts and improved selectivity to NO in the region of light-off. Mesoporous dispersants possess significantly higher surface areas upon which an active phase may be deposited, and have been applied for uranium oxide catalysts [11–13]. Thus far, detailed catalytic information regarding NO reduction and CO oxidation by uranium catalysts has not been presented. Previous investigations utilising amorphous supports have consistently shown that silica provides poorer catalysts [8,9] to Al<sub>2</sub>O<sub>3</sub> or TiO<sub>2</sub>.

The support structure may affect how these materials maintain an active phase [14]. The uranium catalysts supported on

the mesoporous silica H<sub>1</sub>-SiO<sub>2</sub>, synthesised by templating with non-ionic surfactants as in the method due to Attard et al. [15], show sufficient thermal stability to survive calcination to 1073 K with its tertiary structure largely intact. However, such calcination leads to an extrusion of U<sub>3</sub>O<sub>8</sub> from within the pores. There are significant variations in the manner in which the U<sub>3</sub>O<sub>8</sub> phase develops depending upon the support used. This results in both a considerable variation in the average size of the supported particles and in the preferred polymorphs of U<sub>3</sub>O<sub>8</sub>. In mesoporous silica, a hexagonal phase of U<sub>3</sub>O<sub>8</sub> forms first but is then superseded by the orthorhombic form. On amorphous silica or  $\gamma$ -alumina only the hexagonal form of U<sub>3</sub>O<sub>8</sub> is generally observed [14]. An exception to this is presented by catalysts derived from UCl<sub>4</sub>/ $\gamma$ -alumina, where formation of orthorhombic U<sub>3</sub>O<sub>8</sub> is evident. In this report, we investigate the effects of these structural variations on CO oxidation by O<sub>2</sub> and NO.

## 2. Experimental

Catalysts prepared in the manner previously described [14] were pre-treated and calcined in a microreactor [16]. This reactor

\* Corresponding author. Tel.: +44 2380 593307; fax: +44 2380 593781.

E-mail address: [je@soton.ac.uk](mailto:je@soton.ac.uk) (J. Evans).

<sup>1</sup> Present address: Johnson Matthey Plc, Royston, Hertfordshire, UK.

<sup>2</sup> Present address: ESRF, BP220, Grenoble F-38043, France.

utilises a 20–30 mg sample charge held in place by quartz wool plugs and permits the insertion of a 0.5 mm diameter type *k* thermocouple directly into the bed (~5 mm long). Sample heating to 873 K may be achieved using this configuration. Where calcinations have been made to 1073 K microreactor measurements were made ex situ to the calcination. Gases are admitted under mass flow control and the composition of the feedstock measured downstream of the catalyst bed using a quadrupole mass spectrometer station interfaced to the reactor via a stainless steel capillary.

Once loaded into the reactor, samples were thoroughly purged in a He flow prior to exposure to the reactive feedstocks. For CO oxidation experiments, the reactive feedstock comprised a mixture of 5% CO/He and 5% O<sub>2</sub>/He to yield a CO:O<sub>2</sub> ratio of 1:1, with a total flow rate of 20 ml min<sup>-1</sup> (GHSV = 20,000 h<sup>-1</sup>). NO reduction experiments utilised 5% NO/He and 5% CO/He gas mixtures over a range of NO:CO space velocities (ca. 8800–180,000 h<sup>-1</sup>). Typically, the performance of these catalysts was then tested by heating the sample to 873 K at 10 K min<sup>-1</sup> whilst continually monitoring the exit feedstock composition by mass spectrometry. The supported uranium systems were also tested against a more standard 2 wt.% Pt/Al<sub>2</sub>O<sub>3</sub> catalyst (type 4, Johnson-Matthey) using the same weight of catalyst and gas flows.

Individual catalysts and pre-treatment are identified as follows: ucl or unit index the precursor used (UCl<sub>4</sub> or uranyl nitrate, UO<sub>2</sub>(NO<sub>3</sub>)<sub>2</sub>·6H<sub>2</sub>O, respectively); al, si, or h1, index the support material (Degussa Alon C alumina, Grace ES700 silica, and H<sub>1</sub>-SiO<sub>2</sub> mesoporous silica, respectively); lastly nc, or a temperature value detail pre-calcination temperatures (nc = no pre-calcination). For example unit/h1/873 refers to a catalysts derived from uranyl nitrate, supported upon H<sub>1</sub>-SiO<sub>2</sub>, and subjected to a pre-calcination at 873 K.

Based upon a previous study of NO<sub>x</sub> abatement using uranium nitrate derived catalysts supported upon the same  $\gamma$ -alumina [10] (Alon C, Degussa, 100 m<sup>2</sup>g<sup>-1</sup>), all catalysts were made to yield a nominal loading of 30 wt.% U. Only in the case of uranyl nitrate on H<sub>1</sub>-SiO<sub>2</sub> supports was the dependence of catalytic performance upon U loading investigated more closely in the range 0 wt.% < U < 47.5 wt.%. PXRD data was collected as previously described [14] and UO<sub>x</sub> crystallite sizes derived using the Scherrer formula [17].

### 3. Results

Catalytic activity for CO oxidation was displayed by a wide range of the materials synthesised (Fig. 1). A silica supported catalyst of comparable activity to the more usual alumina supported variants was formed from uranyl nitrate on the mesoporous silica without any pre-calcination. This same material proved to be the most active one found for NO reduction by CO (Fig. 2). For Cl free systems, the removal of any pre-calcination step resulted generally in a lower “light-off” temperatures and more active catalysts, the effect being most significant for NO reduction by CO. The net selectivity to N<sub>2</sub>O and N<sub>2</sub> obtained from the catalyst found to be the most active (uncalcined 30 wt.% uranyl nitrate/H<sub>1</sub>-SiO<sub>2</sub>) is comparable to that derived from

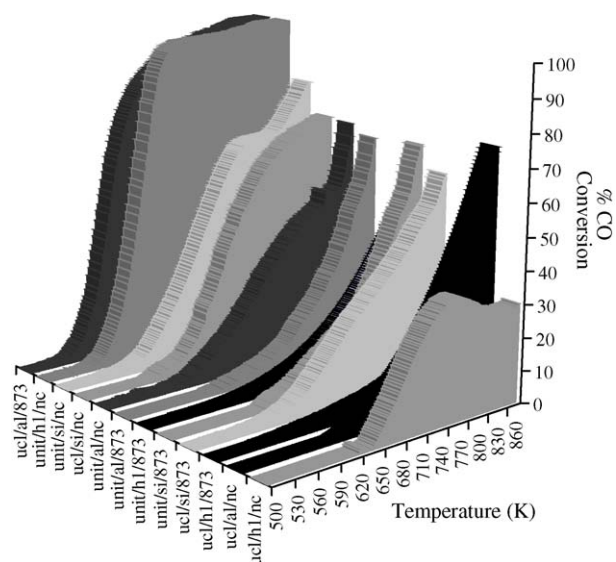


Fig. 1. CO conversion as a function of temperature for a range of supported uranium oxide catalysts, varying by precursor, support and pre-calcination, under a net oxidising (10 ml min<sup>-1</sup> 5% CO, 5 ml min<sup>-1</sup> O<sub>2</sub>, 5 ml min<sup>-1</sup> He: O<sub>2</sub>/CO = 10: GHSV = 20,000 h<sup>-1</sup>) feedstock, and a linear heating ramp of 10 K min<sup>-1</sup>.

the standard Pt/Al<sub>2</sub>O<sub>3</sub> catalyst, particularly in the temperature region of reaction light-off (Fig. 3).

Pre-calcination was beneficial for one of the most active materials (UCl<sub>4</sub>/Al<sub>2</sub>O<sub>3</sub>) for CO oxidation (Fig. 1), and there was also a significant variation in activity as a function of pre-calcination temperature for the CO/NO reaction (Fig. 4). Pre-calcination of this uranium material on the non-porous alumina at 873 K results in an optimal catalyst for CO removal. This corresponds to the minimum temperature required for chlorine removal

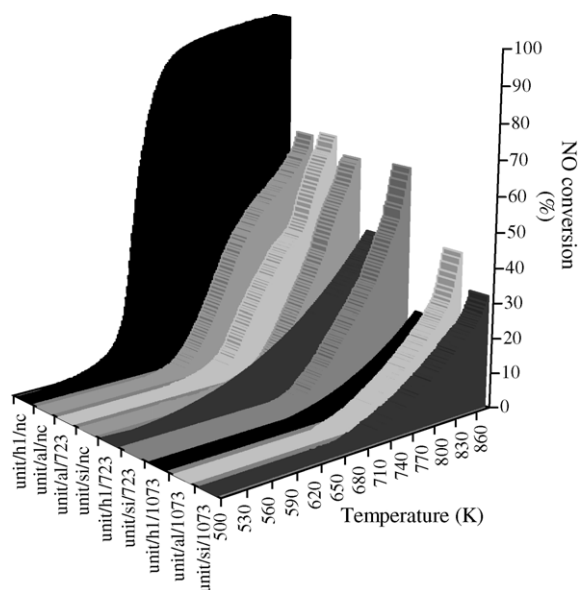


Fig. 2. %NO conversion achieved over 30 wt.% uranyl nitrate derived, H<sub>1</sub>-SiO<sub>2</sub> (black), ES70 (dark grey)  $\gamma$ -Al<sub>2</sub>O<sub>3</sub> (light grey) supported catalysts. Ordinal text labels denote pre-treatment applied: no pre-calcination, pre-calcination in air to 723 K/3h, and 1073 K/3h. Reaction conditions: 10 ml min<sup>-1</sup> 5% NO/He + 10 ml min<sup>-1</sup> 5% CO/He: GHSV = 20,000 h<sup>-1</sup>; linear heating ramp of 10 K min<sup>-1</sup>.

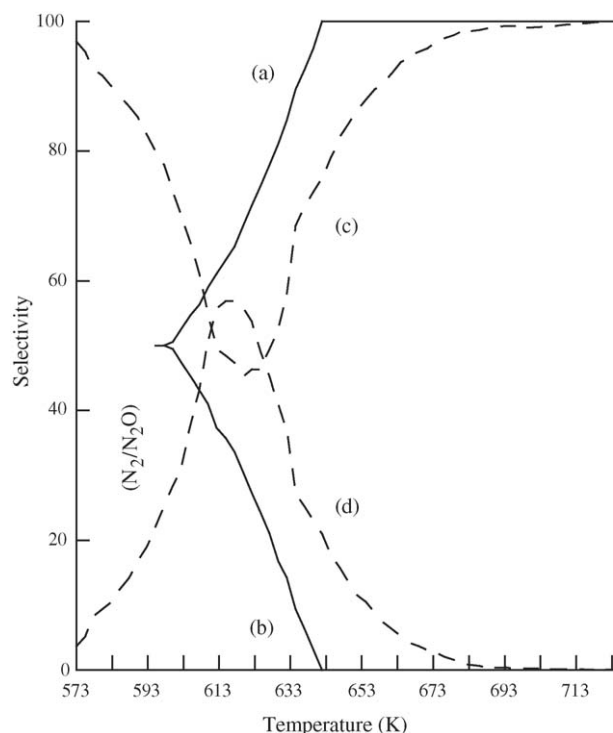


Fig. 3. Selectivity toward  $N_2$  and  $N_2O$  production during NO reduction by CO for the most active uranium oxide system (unit/h1/nc) compared to that derived from a 2 wt.% Pt/ $Al_2O_3$  standard catalyst. (a)  $N_2$  selectivity (unit/h1/nc); (b)  $N_2O$  selectivity (unit/h1/nc); (c)  $N_2$  selectivity (Pt/ $Al_2O_3$ ); (d)  $N_2O$  selectivity (Pt/ $Al_2O_3$ ).

and the onset of  $U_3O_8$  crystallites (of  $\sim 20$  nm domain size) [14].

The structural aspects of the active most active mesoporous material were investigated further. The pore size distribution (Dollimore-Heal method [18] (Fig. 5)) and surface area of the as-made  $H_1$ -SiO<sub>2</sub> support (A) are both reduced after pre-calcination of the unloaded mesoporous support to 1073 K (B). Loading the

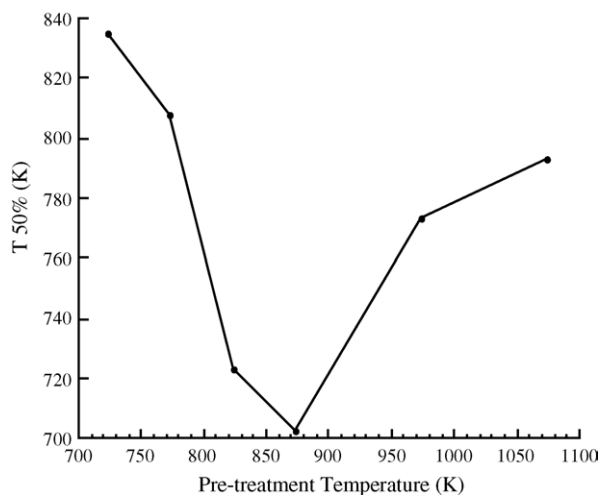


Fig. 4. Variation in the temperature at which 25% NO conversion is achieved ( $T_{50\%}$ ) over  $UCl_4/Al_2O_3$  catalysts, under a  $10 \text{ ml min}^{-1}$  5% NO/He +  $10 \text{ ml min}^{-1}$  5% CO/He ( $GHSV = 20,000 \text{ h}^{-1}$ ) feedstock and a linear heating ramp of  $10 \text{ K min}^{-1}$ , as a function of pre-calcination temperature.

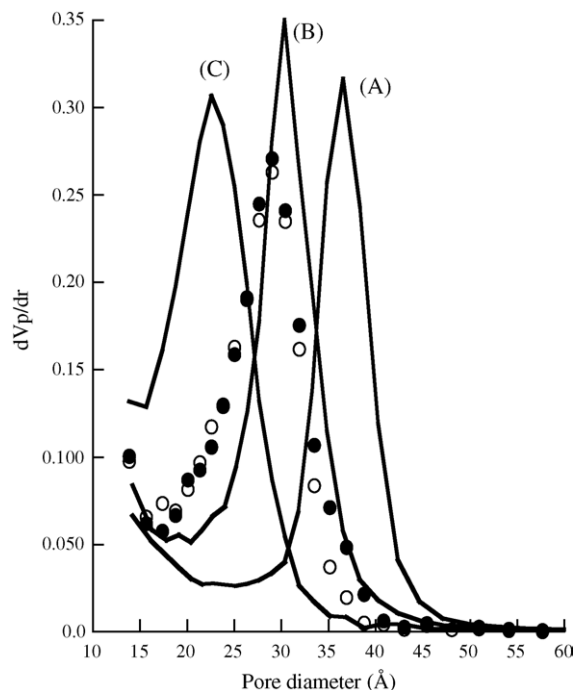


Fig. 5. Ex situ pore size distributions for differently pre-treated  $H_1$ -SiO<sub>2</sub> samples: (A) as prepared ( $BET = 870 \text{ m}^2 \text{ g}^{-1}$ ); (B) unloaded, after calcination in air at 1073 K/3 h ( $BET = 590 \text{ m}^2 \text{ g}^{-1}$ ); (C) after loading with 30 wt.% uranyl nitrate, no pre-treatment ( $BET = 313 \text{ m}^2 \text{ g}^{-1}$ ); filled circles; unit/h1/1073 post CO/NO reaction to 873 K ( $BET = 195 \text{ m}^2 \text{ g}^{-1}$ ); open circles; unit/h1/nc post CO/NO reaction to 873 K/3 h ( $BET = 221 \text{ m}^2 \text{ g}^{-1}$ ).

$H_1$ -SiO<sub>2</sub> with 30 wt. % uranyl nitrate (C) caused larger reduction in both pore diameter and surface area, consistent with there being an internal coating of the mesopores. The two other pore size distributions were derived ex situ after reaction under the 2.5% CO/2.5% NO/95% He. One is derived from a catalyst pre-calcined to 1073 K prior to catalytic study and results in a poor catalyst (Fig. 1); the second, uncalcined catalyst was the most active uranium catalyst. Whether pre-calcined to 1073 K or allowed to evolve under the reactive feedstock to 873 K, the pore size distributions derived ex situ were extremely similar, with an average pore diameter of 28 Å. So the large variations in catalytic activity are not due to any changes in the mesoporous structures.

Fig. 6 shows a powder X-ray diffraction pattern from a 30 wt.% uranyl nitrate/ $H_1$ -SiO<sub>2</sub> catalyst pre-calcined to 873 K and then reacted to 873 K under the CO/NO feedstock. This pattern differs from any measured pre-catalysis [14] or in similar previous studies [10]. The uranium present post reaction is not as  $U_3O_8$  or  $U_4O_9$ , but this pattern most closely resembles is  $U_5O_{11}$  ( $UO_{2.2}$ ) [19,20].

The activity of this chlorine-free  $UO_x$  supported on  $H_1$ -SiO<sub>2</sub> shows a broad maximum between 20 and 30 wt.% loadings (Fig. 7) with a  $T_{50\%} \sim 200$  K lower than that of pure  $U_3O_8$  (47.5 wt.% U). At loadings lower than 20 wt.% catalytic performance gradually deteriorates, both in terms of overall activity and of selectivity (not shown); at loadings of 5 wt.% U or less, increasingly significant contributions from support materials resulted in increasing proportion of  $N_2O$  being formed. A direct

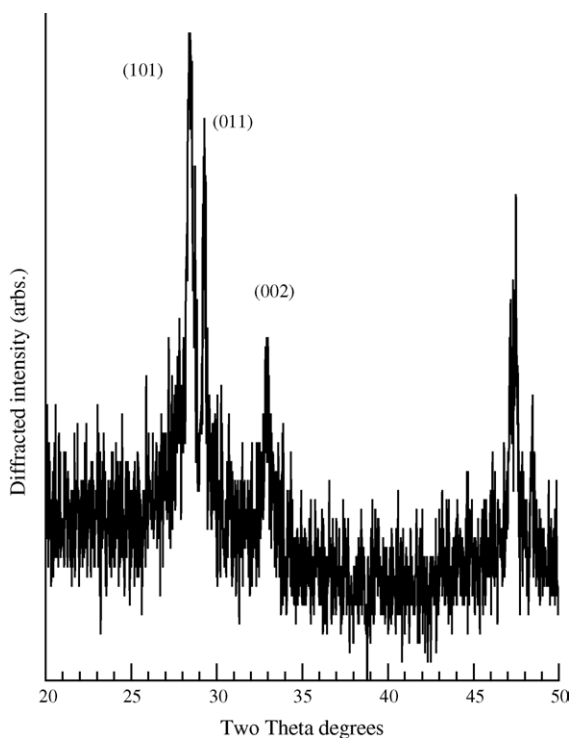


Fig. 6. Powder X-ray ray diffraction (PXRD) pattern from uranyl nitrate/ $\text{H}_1$ - $\text{SiO}_2$  catalyst (calcined at 873 K) derived at room temperature after NO reduction by CO to 873 K.

comparison with the standard  $\text{Pt}/\text{Al}_2\text{O}_3$  catalyst (Fig. 8) shows that the uranyl nitrate based system is the rather less active across the range of contact times investigated. However, over most of the range of contact times, the differential is small (ca. 25 K). Only at the shortest contact times tested did the conversion performance of the Pt catalyst become significantly the better, such that below a contact time of  $0.05 \text{ s}^{-1}$  ( $\text{GHSV} = 72,000 \text{ h}^{-1}$ ) the

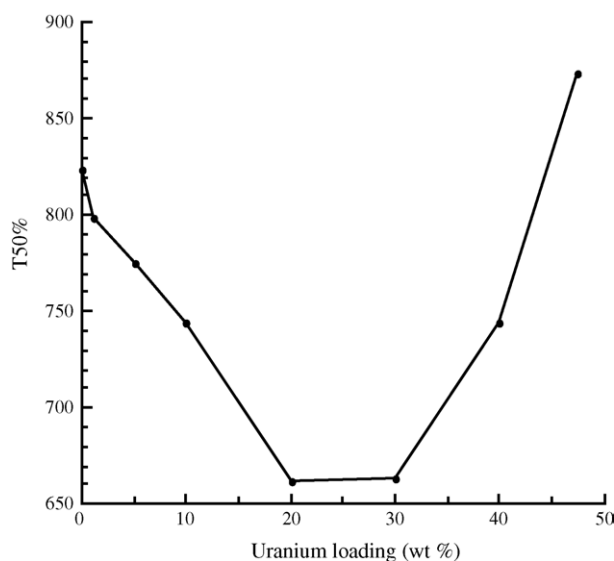


Fig. 7. The dependence upon uranium loading of the net activity of the  $\text{H}_1$ - $\text{SiO}_2$  supported uranyl nitrate based catalysts (uncalcined) for NO reduction by CO. Reaction conditions:  $10 \text{ ml min}^{-1}$  5% NO/He +  $10 \text{ ml min}^{-1}$  5% CO/He;  $\text{GHSV} = 20,000 \text{ h}^{-1}$ ; linear heating ramp of  $10 \text{ K min}^{-1}$ .

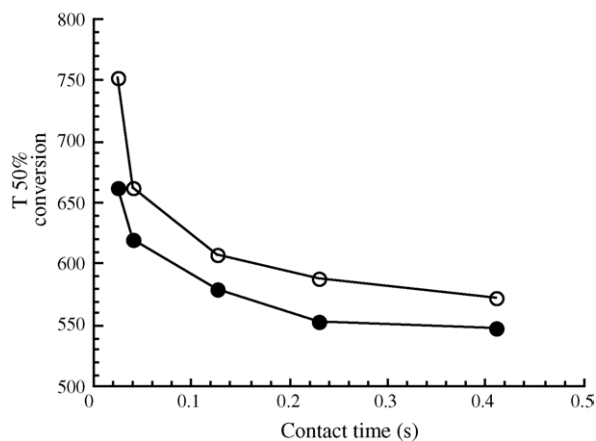


Fig. 8. Comparison of the temperature at which 50% NO is achieved for uranyl nitrate derived,  $\text{H}_1$ - $\text{SiO}_2$  supported catalysts (unit/h/nc, open circles) against that derived from a 2 wt.%  $\text{Pt}/\text{Al}_2\text{O}_3$  catalyst (filled circles), as a function of contact time ( $\text{s}^{-1}$ ).

difference in T 50% between the systems increases to  $\sim 75 \text{ K}$  at  $0.02 \text{ s}^{-1}$ .

Estimates of the apparent activation energy ( $E_{(a)}$ ) and pre-exponential factor ( $\nu$ ) for both catalytic reactions were made from Arrhenius plots of the CO or NO conversion curves in regions of low conversion ( $<20\%$ ) (Fig. 9). By way of reference, the performance of bulk  $\text{U}_3\text{O}_8$  was also measured for both reactions and analysed for kinetic parameters in the same way. The values of  $E_{(a)}$  and  $\nu$  were highly correlated: the most active systems yielded the highest activation energies (Fig. 10). This compensation effect [21] afforded the most active catalysts the highest values of  $\nu$ . The errors associated with  $E_{(a)}$  and  $\nu$  are estimated as ca.  $\pm 10\%$  and  $\pm 20\%$ , respectively, so the relationship between these two kinetic parameters for CO oxidation and NO reduction can be regarded as very similar.

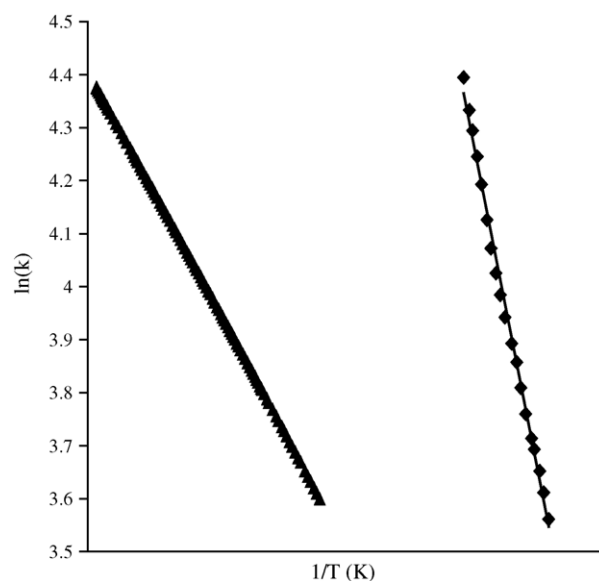


Fig. 9. Representative Arrhenius plots for CO oxidation and NO reduction over differing  $\text{H}_1$ - $\text{SiO}_2$  supported uranium catalysts: (a) unit/h/1073; (b) unit/h/nc.

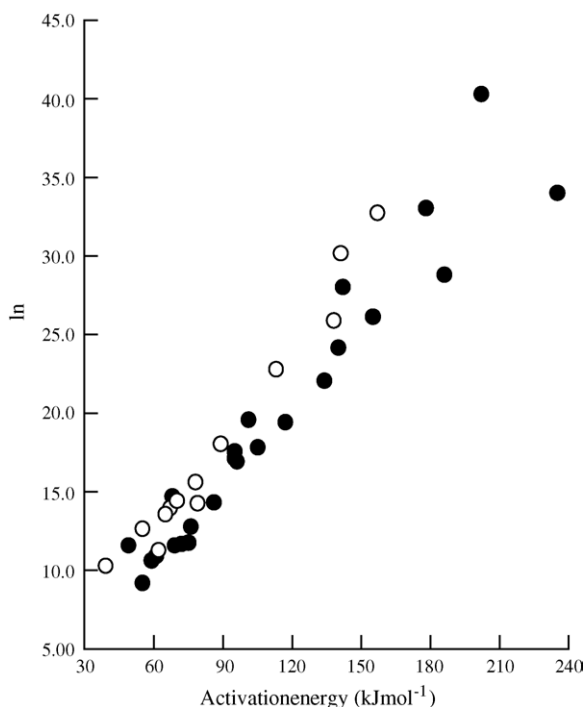


Fig. 10. Variation of  $\ln(v)$  with  $E_{(a)}$ , derived from Arrhenius analysis of the CO and NO conversion over all the catalysts investigated. Filled circles, NO reduction; open circles, CO oxidation.

The relationship between the rate constant at 723 K for NO reduction by CO per unit area and the domain size of the  $\text{UO}_{2.2}$  was investigated for the uranyl nitrate (Fig. 11a) and  $\text{UCl}_4$  (Fig. 11b) derived catalysts on the three types of support. The performance of bulk  $\text{U}_3\text{O}_8$  for NO reduction is also indicated. The most active system for this conversion, unit/h1/nc, outperformed the conventionally preferred alumina based sys-

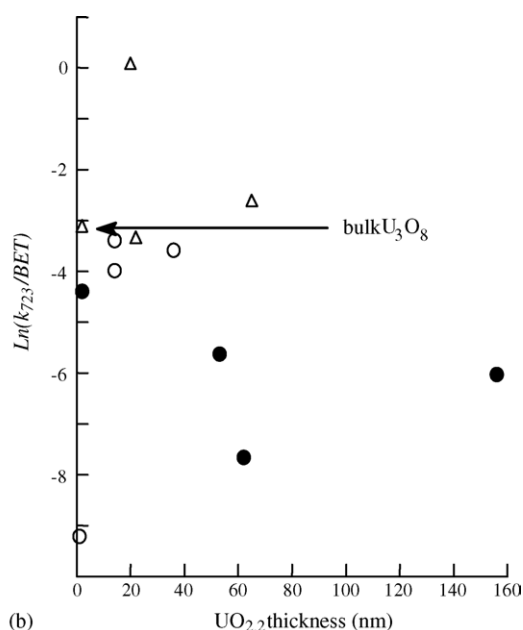
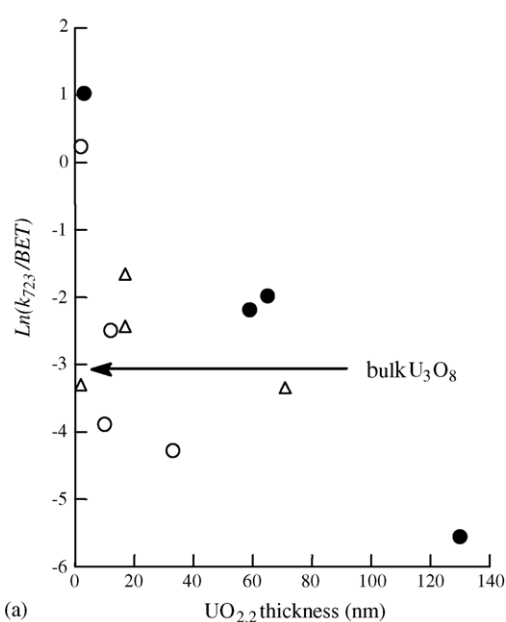


Fig. 11. (a)  $\ln(k^{723}/\text{BET})$  vs. PXRD derived  $\text{U}_5\text{O}_{11}$  average crystallite thicknesses for NO reduction by CO derived from differing precursors and pre-treatments. Filled circles,  $\text{H}_1\text{-SiO}_2$ ; open circles, ES70; triangles,  $\gamma\text{-Al}_2\text{O}_3$ . Catalysts derived from (a) uranyl nitrate and (b)  $\text{UCl}_4$ .

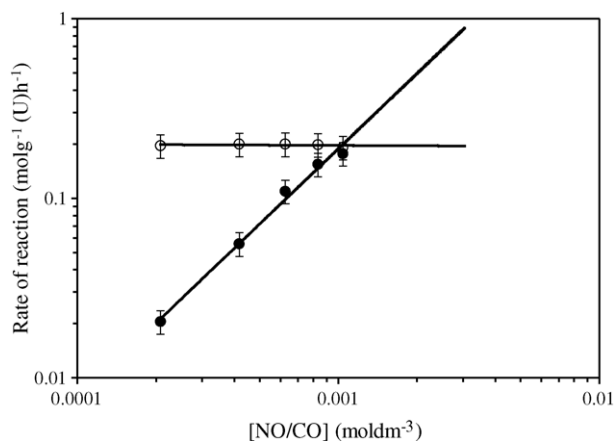


Fig. 12. Rates of reaction vs. NO/CO ratio during NO reduction by CO over the uncalcined uranyl nitrate/ $\text{H}_1\text{-SiO}_2$  catalyst. Open circles, NO variation; filled circles, CO variation.

tems. The generally deleterious effect of Cl on the amorphous and mesoporous  $\text{SiO}_2$  can clearly be seen, especially where no pre-calcination step has been undertaken. In terms of the best catalysts derived from the  $\text{UCl}_4$  precursor, the situation is now inverted with the alumina based systems, calcined up to 873 K, showing the highest activity.

The order of NO reduction with respect to CO and NO was investigated for the unit/h1/nc catalyst (Fig. 12). These results afforded the total rate expression for this reaction of:

$$r = k[\text{CO}]^{1.4} \quad (1)$$

which compares to that derived previously for the same reaction catalysed by bulk  $\text{U}_3\text{O}_8$  [8]:

$$r = k[\text{CO}][\text{NO}]^{0.4} \quad (2)$$

The net order in both cases is the same but in the mesoporous case the total order is now determined solely by the CO component.

#### 4. Discussion

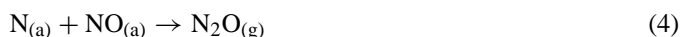
The ability of supported uranium oxide catalysts to facilitate the catalytic oxidation of CO and the selective reduction of NO varies greatly with support, precursor and preparative methodology. In the case of the H<sub>1</sub>-SiO<sub>2</sub> supported catalysts, the methods of catalyst pre-treatment appear to dominate. Silicas have been considered as poor dispersants for an active phase [4,8–10], but by avoiding a pre-calcination stage in the preparation, silicas become considerably superior supports than alumina. The increased activity of these systems is maintained even when they are reacted to 873 K.

The principal reason for this appears to be that this protocol maintains a lower oxidation number of the uranium and avoids large scale sintering of the supported UO<sub>x</sub> phase, thereby maintaining high dispersion and activity (Fig. 11a). Avoidance of pre-calcination also allows containment of the supported uranium oxide within the mesopores of the silica. Developing the catalyst under the reactive feedstock (CO/O<sub>2</sub>/He or CO/NO/He), overcomes the problem of active phase extrusion [14]. However, avoiding the pre-calcination step in alumina supported catalysts also results in small UO<sub>x</sub> domain sizes but fails to elicit superior performance.

For the uranyl nitrate/H<sub>1</sub>-SiO<sub>2</sub> catalyst the rate of NO reduction by CO is independent of [NO], unlike for bulk U<sub>3</sub>O<sub>8</sub> [8]. Hence in this mesoporous catalyst dissociation of NO has been made relatively easier. In terms of surface species, the formation of N<sub>2</sub>O can occur in two ways: the disproportionation of two molecularly adsorbed NO species, i.e.:



or the reaction of an adsorbed NO molecule with an adsorbed nitrogen species left from a previous dissociation event, i.e.:



If NO dissociation has been facilitated so no molecular surface NO species adsorbed at defect sites on the oxide surface exist for an appreciable time, N<sub>2</sub>O formation may only now occur via an Eley-Rideal type interaction of a gas phase NO molecule with an adsorbed N atom before the latter has the chance to find a second N<sub>(a)</sub> species with which to recombine and desorb as N<sub>2</sub>. The high selectivity to N<sub>2</sub> formation indicates the recombination is the faster process under the conditions studied.

The ex situ diffraction characterisation of samples after catalysis indicate a lower oxygen content than U<sub>3</sub>O<sub>8</sub> and the presence of a phase of uranium oxide not previously seen on alumina supported catalysts, namely UO<sub>2.2</sub> [10]. The stoichiometry of this phase is consistent with the range proposed by Wells et al. [10] for the active phase of uranium oxide present supported on γ-Al<sub>2</sub>O<sub>3</sub> (i.e. UO<sub>x</sub>, 2 < x < 2.25). In situ XRD in these alumina based systems, however, only showed the presence U<sub>3</sub>O<sub>8</sub> and

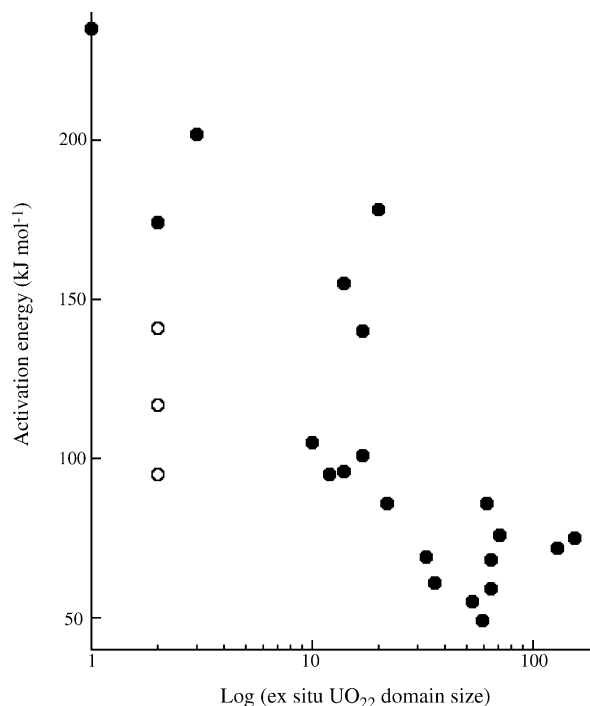


Fig. 13. Variation of the net  $E_{(a)}$  derived for NO reduction by CO as a function of ex situ UO<sub>2.2</sub> (logarithmic axis) domain size for all catalysts studied: open circles are uncalcined systems (nc) with UCl<sub>4</sub> as precursor.

UO<sub>2</sub> during NO reduction by CO. This lower oxygen content in this study may be expected to facilitate the dissociation of adsorbed NO.

The compensation effect between  $\ln(\nu)$  and  $E_{(a)}$  is essentially identical for both CO oxidation and NO reduction, indicating that the rate of dissociation of the oxidant species has become facile enough so that no term containing [NO] or [O<sub>2</sub>] is present in the rate expression. The  $E_{(a)}$  values therefore pertain to the abstraction of surface framework oxygen from the active phase by CO. Per site therefore, the most active systems possess the least reducible supported uranium oxide phases. These  $E_{(a)}$  values for the NO/CO reaction correlate with the logarithm of the UO<sub>2.2</sub> domain size (Fig. 13) and with the pre-exponential factor. Thus increasing the crystallite size of the UO<sub>2.2</sub> may ease the loss of oxygen at a particular site, but these sites will be of reduced availability.

The three cases that deviate most from this general observation (open circles in Fig. 13) have UCl<sub>4</sub> as the precursor and no pre-calcination step. In the alumina case, which has been investigated in most detail with regard to levels of Cl retained after calcination, we can see that the activity maximum in these systems (for CO oxidation and NO reduction) corresponds to the situation wherein the complete loss of Cl from the system has occurred but a relatively small average U<sub>3</sub>O<sub>8</sub> crystallite size is retained; calcination in excess of this temperature (873 K) resulting in ever larger, more poorly dispersed and less reactive systems [14]. The high activity of the ucl/al/873 system occurs at the confluence of these two factors.

Chlorine retention appears to interfere with the active sites formed by small U<sub>3</sub>O<sub>8</sub> particles. A similar result has been

previously reported regarding the activity of Rh/ceria/zirconia catalysts [22,23]. Chlorine retention, promoted by low temperature pre-treatment, was shown, in that case, to lead to a decreased vacancy population and activity, similar to the pattern reported here. In terms of the  $E_{(a)}$  for CO abstracting oxygen from the uranium oxide phase, the deleterious affect of Cl is not significant outside of the three examples where no pre-calcination has been employed. Our previous work [14] has shown that Cl removal (at least from the alumina based systems) starts to proceed at the lowest calcination temperature (723 K) and is completed by 873 K. Moreover, thermogravimetric analyses, coupled with mass spectrometry, indicate that all major weight loss events have occurred by ca. 700–750 K for all these supports. So after pre-calcination (at 723, 873, and 1023 K) chlorine retention will be relatively low. However, Fig. 11b clearly shows that for the net rate constant for NO reduction by CO, nine of the systems (out of 12) derived from Cl precursors show an activity similar to or less than that of bulk  $U_3O_8$ ; in the Cl-free system this applies to five cases (out of 12). The presence of Cl in the catalyst precursor can have a residual effect even after it has been largely removed.

Lastly, it is clear that, over a wide range of contact times the most active catalysts in this study are almost as efficient as the Pt/ $Al_2O_3$  in activity terms for NO removal. Fifty percent conversion is achieved at only marginally higher temperatures above contact times of 0.1 s (by  $\sim 25$  K) than for the reference Pt catalyst. This differential does increase at higher space velocities.

## 5. Conclusions

Considerable enhancements in the performance of uranium oxide catalysts for both CO oxidation and selective NO removal by CO may be obtained by effective containment of the active phase within a mesoporous silica support. Activating the as-deposited system under the reactive feedstock itself provides a means of achieving this. A uranyl nitrate derived system using the mesoporous silica  $H_1$ - $SiO_2$  maintains performance to 873 K, and out-performs analogous  $Al_2O_3$  based catalysts. This system also shows a performance comparable to that obtained from a typical catalyst based upon Pt/ $Al_2O_3$  over a wide range of contact times.

The kinetics of the CO/NO reaction are modified (relative to bulk  $U_3O_8$  case) in the most active catalysts. Any dependency of NO reduction by CO upon gas phase NO concentration is absent in these supported systems. Moreover, the most active systems for both reactions are found to display the highest activation energies (for abstraction of oxygen by CO). Both activation energy and  $\ln(\nu)$  vary logarithmically with crystallite size and are therefore closely correlated to dispersion. However, this is more than compensated for by large increases in pre-exponential factor, pointing to the effectiveness of the increased surface area of the mesoporous support in increasing the frequency of occurrence of active sites.

The incorporation of Cl in the catalyst formulation is generally deleterious to the performance of silica based. However, in one  $Al_2O_3$  supported case (for CO oxidation) the use of a  $UCl_4$

precursor does result in a catalyst that is of comparable activity to even the best uranyl nitrate based system. This promotion coincides with the complete removal of Cl from this just prior to sintering of the  $U_3O_8$  phase to relatively large and inactive particles.

## Acknowledgements

BNFL and the EPSRC are thanked for funding a PhD studentship to TJC and the EPSRC are for postdoctoral funding to MAN. We are also extremely grateful to Professor G.C. Allen and Dr. K.R. Hallam (University of Bristol Interface Analysis Centre) for their advice in interpreting the ex situ PXRD data.

## References

- [1] V. Corberan, A. Corma, G. Kremenec, *Ind. Eng. Chem. Prod. Res. Dev.* 24 (1984) 546;  
V. Corberan, A. Corma, G. Kremenec, *Ind. Eng. Chem. Prod. Res. Dev.* 24 (1985) 62.
- [2] J.L. Callahan, B. Gertissier, US Patent 308,151 (1965);  
J.L. Callahan, B. Gertissier, US Patent 198,750 (1967).
- [3] J.C. Steenhof de Jong, C.H.E. Guffens, H.F.S. Van der Baan, *J. Catal.* 26 (1972) 401;  
J.C. Steenhof de Jong, C.H.E. Guffens, H.F.S. Van der Baan, *J. Catal.* 31 (1973) 127.
- [4] H. Collette, V. Deremince-Mathieu, Z. Gabelica, J.B. Nagy, E.G. Derouane, J.J. Verbist, *J. Chem. Soc. Faraday Trans.* 83 (1987) 1263.
- [5] G.J. Hutchings, C.S. Heneghan, I.D. Hudson, S.H. Taylor, *Nature* 384 (1996) 341.
- [6] F. Nozaki, K. Ohki, *Bull. Chem. Soc. Jpn.* 45 (1972) 3473.
- [7] F. Nozaki, M. Kobayashi, S. Yoshida, *Nippon Kagaku Kaishi* 26 (1972).
- [8] F. Nozaki, F. Matsukawa, Y. Mano, *Bull. Chem. Soc. Jpn.* 48 (1975) 2674.
- [9] H. Collette, S. Maroie, J. Riga, J.J. Verbist, Z. Gabelica, J.B. Nagy, E.G. Derouane, *J. Catal.* 98 (1986) 326.
- [10] S.D. Pollington, A.F. Lee, T.L. Overton, P.J. Sears, P.B. Wells, S. Hawley, I.D. Hudson, D.F. Lee, V. Ruddick, *Chem. Commun.* (1999) 725.
- [11] Z.T. Zhang, M. Konduru, S. Dai, S.H. Overbury, *Chem. Commun.* (2002) 2406.
- [12] (a) D. Kumar, G.K. Dey, N.M. Gupta, *Phys. Chem. Chem. Phys.* 5 (2003) 547;  
(b) D. Kumar, S. Bera, A.K. Tripathi, G.K. Dey, N.M. Gupta, *Micropor. Mesopor. Mater.* 66 (2003) 157.
- [13] R. Tismaneanu, B. Ray, R. Khalifin, R. Semiat, M.S. Eisen, *J. Mol. Catal. A* 171 (2001) 229.
- [14] T. Campbell, M.A. Newton, V. Boyd, D.F. Lee, J. Evans, *J. Phys. Chem. B* 109 (2005) 2885.
- [15] G.S. Attard, J.C. Glyde, C.G. Göltner, *Nature* 378 (1995) 366.
- [16] S.G. Fiddy, M.A. Newton, A.J. Dent, G. Salvini, J.M. Corker, S. Turin, T. Campbell, J. Evans, *Chem. Commun.* (1999) 851.
- [17] P. Scherrer, *Nachr. Göttinger Gessell.* (1918) 98.
- [18] D. Dollimore, G.R. Heal, *J. Appl. Chem.* (1964) 109.
- [19] I. Zvesdinskaya, L. Dubrivinskiy, *Dokl. Acad. Sci. USSR Earth Sci. Sec.* 319 (1993) 197 (English translation).
- [20] G.C. Allen, K.R. Hallam, Private communication.
- [21] For instance M. Boudart, G. Djega-Mariadassu, *Kinetics of Heterogeneous Catalytic Reactions*, Princeton University Press, Princeton, 1984, p. 124.
- [22] P. Fornasiero, N. Hickey, J. Kaspar, C. Dossi, D. Gava, M. Graziani, *J. Catal.* 189 (2000) 326.
- [23] P. Fornasiero, N. Hickey, J. Kaspar, T. Montini, M. Graziani, *J. Catal.* 189 (2000) 339.